VOL. 10, NO. 9, MAY 2015 ISSN 1819-6608
ARPN Journal of Engineering and Applied Sciences


www.arpnjournals.com

A NOVEL SENSING NOISE AND GAUSSIAN NOISE REMOVAL METHODS VIA SPARSE REPRESENTATION USING SVD AND COMPRESSIVE SENSING METHODS

D. Regan[1] and S. K. Srivatsa[2]
[1]St. Peter's University, Avadi, Chennai, India
[2]Anna University, Chennai, Tamil Nadu, India

ABSTRACT

Image processing is one of the common research areas in recent decades, since noisy images cause harmful consequence on several applications and considerably degrade visual quality. The term denoising indicates to the method of estimating the unidentified (original) signal from available noisy data. Hyperspectral imaging has been established that it has several applications in farming, diagnostic medicine, and military surveillance. On the other hand, in these applications, the occurrence of the noise considerably reduces the classification accuracy. In order to solve these setbacks, for HSI, there is much global and local redundancy and correlation (RAC) in spatial/spectral dimensions is proposed in earlier work to eliminate noise from samples. Additionally, denoising performance can be enhanced significantly if RAC is exploited professionally in the denoising process. Nevertheless, the available RAC method denoising performance possibly will decrease when noise is strong. It turns out to be one of the important issues on dictionary learning. With the intention of surpassing these setbacks, in this paper presented a noise removal scheme to eradicate noise from image samples, at first the sensing noise in the image samples are eradicated with the help of the Singular Value Decomposition (SVD) and the Gaussian noise in the image samples are eradicated with the help of the Compression Sensing (CS) methods. SVD algorithm utilizes both the spectral and the spatial information in the images. Noise can be eliminated by sparse approximated data with SVD techniques. The denoising outcome from the proposed method is better than the other hyperspectral denoising schemes. Our results demonstrate that our denoising method can achieve competitive performance than other state-of-the-art methods.

Keywords: global redundancy and correlation (RAC), hyperspectral image (HSI) denoising, local RAC, low rank, sparse representation, singular value decomposition (SVD) , the compression sensing (CS) methods.

1. INTRODUCTION

Hyperspectral images are exploited in several sensible applications, for instance, the exposure of earth surface, soil category examination, farming and forest monitoring, environmental investigations, and military surveillance [1-2]. On the other hand, in applications such as target recognition, the occurrence of the noise considerably reduces the classification accuracy by blurring the outlines of objects of concern. An additional effect of the noise is the lessening of spectral un mixing, in which the noise affects the perfect determination of sporadically occurring end members [3]. In contrast, the hyperspectral sensors are also extremely responsive to the noise owing to their nonlinear reaction in several spectral bands which results in a worsening of captured data quality. As a result, the noise reduction is a vital challenge in hyperspectral images applications.

In recent times, several HSI denoising schemes have been developed [4-6]. The easiest approach is to exploit the conventional 2-D or 1-D denoising techniques to condense noise in HIS band by band or pixel by pixel. But, the related denoising result by this approach is not pleasing, because only spatial or spectral noise is eliminated. In case if noise only reducedin spatial or spectral domain, artifacts or distortions will be established in supplementary domains. Simultaneously, this category of techniques will demolish the correlation in spatial or spectral domain. Spatial and spectral information is supposed to be considered mutually to eliminate the noise efficiently. But, these approaches possibly will lead to loss of information because the correlations among spatial and spectral bands are not concurrently considered.

An integration of spatial and spectral wavelet shrinkage that benefits from the variation of the signal nature in the spatial and spectral dimensions and works in the spectral derivative domain was formulated in [6]. An additional denoising approach [7] diminished the dimensionality of hyperspectral images by means of PCA and concurrently eliminated the noise in the images with the help of bivariate wavelet shrinkage. In fact, bivariate wavelet shrinkage is an extremely efficient approach in image denoising that considers the parent–child coefficient association in the wavelet domain.

In [8], an image restoration in which neighbourhoods of wavelet sub-bands were represented by a discrete mixture of linear projected Gaussian scale mixtures was formulated. This method is also constructive for real-time denoising applications. Some approaches in recent times have considered hyperspectral images as 3-D data which are also regarded as third-order tensor: two spatial dimensions and one spectral dimension. For example,in [9] hyperspectral images were taken as a 3-D tensor and denoising of hyperspectral images in the domain of imaging spectroscopy was achieved by the vectorial anisotropic diffusion.

As a dominant statistical image modelling approach, sparse representation has been productively exploited in image denoising [10-11]. In case of a sparse representation structure, a dictionary can be learned by exploiting the RAC in an image. A noise-free image can be sparsely estimated by dictionaries' atoms, while a noisy image cannot be sparsely estimated owing to noise's stochastic character. The denoised image is estimated with the help of linear combination of atoms or bases. HSI includes multiple images obtained from auninterrupted spectrum with narrow bandwidth, and there is vastdistinction in different band subsets. Extremely correlated images set have the nature of small rank; they can be recovered resourcefully from measurement with noise or outliers by utilizing the restriction of low rank.

In this research work, a new noise reduction method is developed for hyperspectral images with the help of a K-SVD. This technique of denoising can well eliminate a range of mixed or single noise by employing sparse regularization of small image patches. It also preserves the image texture in a comprehensible manner. The learned dictionary exploited undoubtedly helps in eliminating the noise. At the same time,K-SVD accomplished an outstanding compression ratio and noise reduction. The weighted rank-one approximation setback is solved with the help of the new iterative scheme and the low rank approximation can be achieved by SVD and the Gaussian noise in the image samples are eliminated by means of the Compression Sensing (CS) methods.

2. BACKGROUND STUDY

In [6] formulated a spectral and spatial adaptive total variation (TV) denoising method, it recommends that noise intensity is dissimilar in band by band or can say deviation in noise intensity band by band, as a result there should be special technique or the denoising strength should be regulate with deviation in noise intensity in different bands. Therefore to eradicatethis type of deviation in noise, a hyperspectral image denoising algorithm utilizing a spectral–spatial adaptive total variation (TV) model, it takes care of the spectral noise differences and spatial information differences in process on reducing noise. As a result, it enforces the spatial efficiency and spatial discontinuity.

Chen *et al.* [4] developed a denoising approach for hyperspectral images with convincinglybetter SNR by employing principal component analysis and wavelet shrinkage. The algorithm employed PCA to decorrelate the fine features of the data cube from the noise, and subsequentlycondensed the noise only in the noisy low-energy PCA output channels with wavelet shrinkage denoising.

Kotwal *et al.* [12] formulated a bilateral filtering-based approach is developed for hyperspectral image fusion to produce a correct resultant image. This approach keeps even the minor details that arepresent in individual image bands, by using the edge-preserving features of a bilateral filter. It does not introduce noticeable artifacts in the fused image. A hierarchical fusion method has also been formulated by this author for implementation purposes to hold a huge number of hyperspectral image bands. This approach provides computational and storage effectiveness without influencing the quality and performance of the fusion.

Xu *et al.* [13] suggested a noise estimation approach of hyperspectral remote sensing image, which depends on MLR and wavelet transform. This approach eliminates the spatial correlation of the residual image extracted by MLR by means of wavelet transform. Finally,the standard deviation is approximated from the median absolute value of the wavelet coefficients of the noisy signals in the high-frequency subbands.

Acito *et al.* [14] developed anapproach for striping noise reduction in hyperspectral images. This approach makes use of the orthogonal subspace method to approximate the striping component and to eliminate it from the image, preserving the helpful signal. The approach does not introduce artifacts in the data and also considers the dependence on the signal intensity of the striping component.

Letexier *et al.* [15] presented a Multidimensional Wiener Filtering (MWF) approach. It considers a multidimensional data set as a third-order tensor. It also depends on the separability among a signal subspace and a noise subspace. By means of multilinear algebra, MWF requires to flatten the tensor. On the other hand, flattening is always orthogonally carried out, which possibly will not be adapted to data. Indeed, as a Tucker-based filtering, MWF only takes the useful signal subspace into account. When the signal subspace and the noise subspace are extremely close, it is complicated to obtain all the constructive information.

Karami *et al.* [16] formulated new noise reduction approach for the denoising of hyperspectral images. Thapproach, Genetic Kernel Tucker Decomposition (GKTD), makes use of both the spectral and the spatial information in the images. With regard to a previous approach, employ the kernel concept to apply Tucker decomposition on a higher dimensional feature space rather than the input space. A genetic algorithm is exploited to optimize for the lower rank Tucker tensor in the feature space.

Among them all of the methods only reduce noise in spatial or spectral domain, artifacts or distortions will be introduced in other domains. At the same time, this kind of methods will destroy the correlation in spatial or spectral domain.

3. PROPOSED METHODOLOGY

In this paper, a general framework is developed to adaptively identify and eliminate noise of several category, comprising Gaussian noise, impulse noise and more significantly, their combination in the HSI data. The HSI data is regarded as a three order tensor which takes care of both spatial and spectral modes of the particular image. Compressive Sensing (CS) is an approach to recover sparse signals from considerably less measurements than required with the conventional

sampling theory. The image experiences tensor decomposition; in a while the modified K-SVD algorithm is implemented to the tensors. The regularized Maximum Likelihood Estimation (MLE) is customized with new function together with additional variable, because the original likelihood functional associated with mixed noise is not simple to be optimized compared against the functional for a single Gaussian noise. This new functional has the similar global minimizer as the original likelihood functional and is simpler to be optimized. The weighting functions takes the role of noise detectors by reducing the new functional, acquire some weighted norms models. It also incorporates this with sparsity representation, as a result this scheme can well restore images and textures damaged by mixed noise. This scheme comprises of four phases: sparse coding followed by dictionary learning, image reconstruction, noise clustering (detection), and parameters estimation. Each phaserequires to carry out a minimization setback. Then these optimized tensors are partitioned as noise free tensor and noisy tensor. The noise free tensors are then integrated to rebuild the noise free image. The reconstruction is identical as reverse of the tensor decomposition.

a) Model representation

Consider an original Hyperspectral image, and the degradation noise is taken as additive noise, the noise degradation model of the Hyperspectral image is given in the following equation

$$f = u + n \quad (1)$$

Where $u = [u_1, u_2, \dots, u_j \dots, u_B]$represents the original clear Hyperspectral image, with the size of $M \times N \times B$, in which Mindicates the samples of the image, Nrepresents the lines of the image, and B indicates the number of bands. $f = [f_1, f_2, \dots f_j, \dots, f_B]$ represents the noise degradation image which also of size $M \times N \times B$, and $n = [n_1, n_2, \dots, n_j, \dots, n_B]$, indicates the additive noise with the similar size as u and f. Hyperspectral imaging (HSI) gathers and process information from across the electromagnetic spectrum. The human eye notices detectable light in three bands (red, blue, green). Spectral imaging splits the spectrum into several more bands. This approach of segmenting images into bands can be extended before can be extended beyond the visibility. Hyperspectral sensors gather a collection of images. Each image is a range of the electromagnetic spectrum recognized as a spectral band. Subsequently these images are integrated together to generate a three dimensional hyperspectral data cube.

b) Compressive sensing for sparse noise removal

Compressive Sensing (CS) is an approach to recover sparse signals from considerably less measurements than required with the conventional sampling theory (See Figure-1).

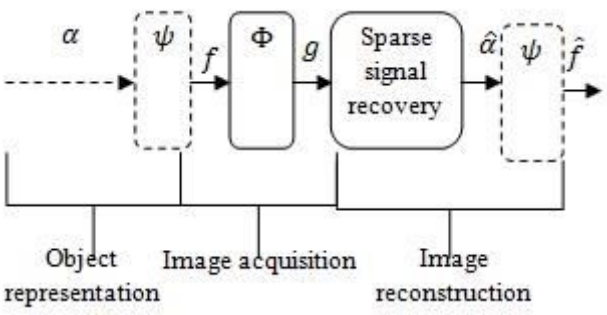

Figure-1. Compressive sensing block diagram.

In the above figure1, $f$indicates a physical signal, e.g. objects intensities. α representsa vector of components in the sparsifying domain exploited to represent f. $\alpha$is a mathematical representation vector that includes largely zeros or close to zero values. In the image acquisition phase, the signal vector f is sampled with the help of the Φ operator yielding the measurement vector g. Subsequently consider that a $N \times 1$ vector f that is to be measured can be given as $= \Psi\alpha$, where the $N \times 1$ vector αincludes only $k << N$ non-zero elements and Ψrepresents a spasrsifying operator. The measurements vector$g \in \mathbb{R}^{M\times 1}$, is obtained by $g = \Phi f$ where $\Phi \in \mathbb{R}^{M\times N}$represents a sensing matrix. By appropriately selecting $M$and Φ, and considering sparsity of $f$in the Ψ domain, the signal f can be recovered from the measurements g. The fundamental step here is to construct a sensing matrix Φin order that it enables perfect recovery of N sized f from fewer M measurements g. Reconstruction off from g is certain when the number of measurements Msatisfies the following criteria: $\geq C\mu^2 Klog(N)$. It can be seen that the number of measurements necessary, M, based on the size of the signal, N, its sparisity, k, and μindicates the mutual coherence among Φ and Ψ. The mutual coherence is given as:

$$\mu(\Phi, \Psi) = \sqrt{M} \max_{1 \leq j,j \leq M} |\langle \Phi_i, \Psi_j \rangle| \quad (2)$$

where Φ_i , Ψ_j are vectors of Φ and Ψcorrespondingly. The value of μ is inside the range of $1 \leq \mu \leq N$. The lesserμ is, the better the performance of the system and superiority of the product. The original signal f can be recovered by solving the following equation

$$\hat{f} = \Psi\hat{\alpha} \text{ subject to } \min_{\hat{\alpha}}\{\|g - \Phi\Psi_\alpha\|_2^2 + \gamma\|\alpha\|_l\} \quad (3)$$

Where, $\gamma\|*\|_l$ is l_1 norm and γ is a regularization weight. One of the complicatedness of utilizing the CS method for HS imaging is the enormous size of matrices Φnecessary for representing the sensing operation. Signals in the CS theory are indicated by vectors with N components. The measurements data is M dimensional; accordingly the sensing matrix is of size$\Phi \in \mathbb{R}^{M\times N}$.

Hyperspectral imaging involves 3D signals $F \in \mathbb{R}^{N_1 \times N_2 \times N_3}$ which can be transformed to vectors by lexicographic ordering to N - length vector$(f = vec(F))$. Since $N = N_1 \times N_2 \times N_3$ the sensing matrix size has the order of$(N_1 \times N_2 \times N_3)^2$. For illustration consider the computational characteristics of random encoding a 3D data HS cube of$F \in \mathbb{R}^{N_1 \times N_2 \times N_3}$, with $N_1 = N_2 = N_3 = 256$. In this scenario, the sensing matrix Φ will be $\Phi \in \mathbb{R}^{2^{24} \times 2^{24}}$. The optical execution and sensor calibration of such systems also face a big challenge since the realization of random Φnecessitates the system to have $N \times M$almost independent modes.

c) Singular value decomposition for noised removal

The Singular Value Decomposition (SVD) is also regarded as the "swiss army knife" of matrix decompositions. Applications of the SVD tend to be changed from Latent Semantic Indexing (LSI) to collaborative filtering. The SVD is also one of the most costly decompositions, both based on computation and memory consumption. Here presented a well-organized algorithm for discovering the SVD for two special groups of matrices: sparse matrices and band matrices. The SVD of a matrix $A \in R^{m \times n}$is given as,

$$A = U\Sigma V^T \tag{4}$$

Where $U \in R^{m \times m}$ and $V \in R^{n \times n}$ and U and V are orthogonal matrices. $\Sigma \in R^{m \times n}$ represents a diagonal matrix with real positive entries. This formulation of the SVD is commonly indicated as the full SVD. The more frequently exploited form of SVD is $A \in R^{m \times n}$ and $m \geq n$ is given as,

$$A = \hat{U}\hat{\Sigma}V^T \tag{5}$$

where$\hat{U} \in R^{m \times n}$ and $V \in R^{n \times n}$ and $\hat{U}$ and V have orthonormal columns. $\hat{\Sigma} \in R^{n \times n}$ representsa diagonal matrix with real positive entries. This is usually called as the thin SVD or the economy SVD. The concept in this paper is relevant to both the thin and full SVD. SVD is used to refer both SVD's and make a distinction wherever required.

d) Matrix SVD for image denoising

Provided a matrix A of size $m_1 \times m_2$, there occurs a factorization of the form,

$$A = USV^T \tag{6}$$

where U is a $m_1 \times m_1$ orthonormal matrix, S is a $m_1 \times m_2$ diagonal matrix of positive 'singular' values and V is a $m_2 \times m_2$orthonormal matrix. The columns of V and the columns of U (correspondingly called the right and left singular vectors) are respectively the eigenvectors of the column-column correlation matrix A^TA and the row-row correlation matrix AA^T. The singular values in S are the square roots of the Eigen values of A^TA (or AA^T). The SVD also provides the optimal low rank decomposition of A, i.e. the optimal solution to,

$$E(\check{A}) = \|A - \check{A}\|^2 \text{ subject to the constraint rank} \tag{7}$$

$$(\check{A}) = k, k < m_1, k < m_2 \tag{8}$$

is given as,

$$\check{A} = \|U_k \check{S} V_k^T\|^2 \tag{9}$$

whereU_k and $V_k$represents the first k columns of U and V respectively and $\check{S}$ includes the k largest singular values of S. The singular values of natural images tend to decompose exponentially and the SVD bases have a frequency interpretation. Provided a noisy image A (a corrupted format of an underlying clean image) influenced by noise from $N(0, \sigma)$, filtering is completed in three phases:

(1) Calculating the decomposition of small patches $A_i = U_i S_i V_i^T$ of size $p \times p$ in sliding window method,

(2) Manipulating the singular values $\{S_i\}$, and

(3) Averaging the hypotheses appearing at each pixel to construct a final filtered image.

The original K-SVD is fine tuned by the non-uniform weights. In that case indicate,

$$W = (R_{1w} \dots R_{Nw}), X = (R_1 f \dots R_N f) \tag{10}$$

Then

$$D^{v_1+1} = \arg \min_{D, \|d_k\|_2 = 1} \{\|D\alpha^{v_1+1} - X^v\|_F^2\} \tag{11}$$

Similar to the K-SVD learning approach is the ordinary approach to reduce each atom d_k as follows:

$$d_k^{v_1+1} = arg \min_{D, \|d_k\|_2 = 1} \|W^{\circ}(E^k - d_k \alpha_{k_r}^{v_1+1})\|_F^2 \tag{12}$$

This is the weighted approximation setback. This is resolved by an iterative approach by means of SVD. This approach cannot be exploited for the unweighted case. As a result, the minimization setback is solved. Hence the modified scheme diminishes the original K-SVD algorithm when all weights are the similar.

Reconstruction

This minimization setback is solved as given below, since $\mathcal{J}$ is quadratic with respect to f, accordingly

$$f^{v+1} = \left(d(\omega \circ \omega) + \lambda \sum_{i=1}^{N} R_i^T d\left((R_i \omega) \circ (R_i \omega) \right) R_i \right)^{-1} \times \left(d(\omega \circ \omega) g + \lambda \sum_{i=1}^{N} R_i^T d\left((R_i \omega) \circ (R_i \omega) \right) R_i \times D^{v+1} \alpha_i^{v+1} \right) \quad (13)$$

Where $(\omega \circ \omega)$ indicates $diag\omega \circ \omega$ and R_is represents adiagonal matrix. Consequently the inverse matrix can be directly obtained. The signal dominant constituents are united by removing the noise tensors. Following the noise components are removed, the noise free image is obtained by rebuilding the signal dominant components. The tensors are rebuilt to form the noise free HIS data by the equation,

$$\hat{S} = \sum_{r=1}^{k} \lambda_r U_r \circ V_r \circ W_r \quad (14)$$

The value of Kindicates the number of signal dominant tensors.

5. EXPERIMENTATION RESULTS

This section will demonstrate the denoising performance of the K-SVD and CS proposed algorithm on simulated and real noisy HSI. In order to evaluate the competitive performance of the proposed method, it is evaluated against the two state-of-the-art methods; one is the global and local redundancyand correlation (RAC) [17], and another one which is an extension of the principal component analysis transform(PCA) [4] to the multichannel image case. Evaluation is done on three data sets; they are synthetic HSI using USGS spectral library (as shown in Figure-2), Sandi go, and Washington DC Mall data. In view of the fact that certain spectral bands of the latter two datasets are affected by noise largely, they cannot be exploited as ground truth. Then obtain numerous continuous bands that are free from noise to be ground truth by visual assessment. The synthetic HSI has a size of $75 \times 75 \times 224$; size of the two latter data subsets is $256 \times 256 \times 68$. The assessing indexes employed are Peak Signal-to-Noise Ratio (PSNR), Structural Similarity Index Measurement (SSIM) [18], and Feature Similarity Index Measurement (FSIM) [19]. The latter two indexes are intended depending on human's visual quality. Index value is higher; denoised image is more comparable to the original image in human' svision sense.

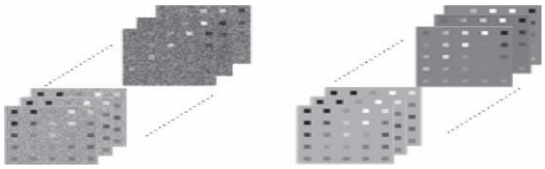

Figure-2. Simulated HSI [20] by using the spectral signature selected from USGS library with a size of $75 \times 75 \times 224$

The left is noise free, and its rank is 5. The right HSI is degraded by noise with zero mean and standard variance of 10, and its rank is full (Rank = 224).Numerical experimentations are carried out on these three data sets under various noise levels. All the indexes PSNR, SSIM, and FSIM are calculated for images on different spectral bands; the mean of these bands are then computed and indicated as MPSNR, MSSIM, and MFSIM. Assessing indexes of the experiment on synthetic HSI by means of USGS library are given in Table-1.

Table-1. Assessing indexes of different denoising algorithms on synthetic HSI data using USGS spectral library under different noise levels.

Noise level	Assessing indices	Inputting noisy image	PCA	RAC	CS-K-SVD
σ = 0.05	MPSNR(db)	28.0261	40.3641	41.9264	42.268
	MSSIM	0.2712	0.8236	0.8895	0.9587
	MFSIM	0.9072	0.9792	0.9854	0.9878
σ = 0.10	MPSNR(db)	20.0018	35.325	37.851	38.5968
	MSSIM	0.1598	0.6235	0.7832	0.8124
	MFSIM	0.8698	0.9578	0.9658	0.9785
σ = 0.15	MPSNR(db)	16.4806	33.2568	36.589	37.5897
	MSSIM	0.1109	0.4869	0.6782	0.7895
	MFSIM	0.8518	0.9482	0.9568	0.9785
σ = 0.20	MPSNR(db)	13.3812	32.1568	32.8954	33.5689
	MSSIM	0.1008	0.42156	0.6897	0.7895
	MFSIM	0.8420	0.9458	0.9684	0.9728
σ = 0.25	MPSNR(db)	12.0430	26.989	32.5698	36.589
	MSSIM	0.0894	0.3289	0.4812	0.5248
	MFSIM	0.8361	0.9207	0.9456	0.9547

The visual superiority of the denoised images to the results of other approaches is also clear. Alike conclusion can be made in the experiment on Sandi go data (see Table-2) and in the experiment on Washington DC Mall data (see Table-3). The proposed scheme offers competitive result to the state-of-the-art approaches.

Table-2. Assessing indexes of different denoising algorithms on Sandi go data under different noise levels.

Noise level	Assessing indices	Inputting noisy image	PCA	RAC	CS-K-SVD
σ = 0.05	MPSNR(db)	34.1871	40.7128	41.4389	42.6897
	MSSIM	0.9303	0.9837	0.9908	0.9928
	MFSIM	0.9708	0.9909	0.9936	0.9968
σ = 0.10	MPSNR(db)	28.1260	37.8598	38.4612	38.5968
	MSSIM	0.7791	0.9717	0.9788	0.9823
	MFSIM	0.9176	0.9825	0.9887	0.9912
σ = 0.15	MPSNR(db)	23.6097	35.4287	36.0729	37.5897
	MSSIM	0.6729	0.9587	0.9678	0.9784
	MFSIM	0.8612	0.9778	0.9829	0.9879
σ = 0.20	MPSNR(db)	22.1478	33.7249	34.0789	35.7897
	MSSIM	0.5924	0.9330	0.9587	0.9687
	MFSIM	0.8214	0.9682	0.9758	0.9849
σ = 0.25	MPSNR(db)	20.1649	32.1479	32.4579	33.8794
	MSSIM	0.5389	0.9078	0.9487	0.9687
	MFSIM	0.7847	0.9587	0.9678	0.9712

Table-3. Assessing indexes of different denoising algorithms on Washington DC mall data under different noise levels.

Noise level	Assessing indices	Inputting noisy image	PCA	RAC	CS-K-SVD
σ = 0.05	MPSNR(db)	34.1780	41.0601	42.2457	43.1548
	MSSIM	0.9382	0.9848	0.9925	0.9956
	MFSIM	0.9797	0.9956	0.9978	0.9984
σ = 0.10	MPSNR(db)	28.1118	37.3548	38.1687	38.5968
	MSSIM	0.79438	0.9748	0.9840	0.9912
	MFSIM	0.9325	0.9911	0.9924	0.9943
σ = 0.15	MPSNR(db)	24.6163	35.4287	35.9874	37.5897
	MSSIM	0.7242	0.9587	0.9754	0.9894
	MFSIM	0.9004	0.9778	0.9784	0.9814
σ = 0.20	MPSNR(db)	20.1478	33.7249	33.0789	35.7897
	MSSIM	0.6387	0.9387	0.9587	0.9646
	MFSIM	0.8647	0.9775	0.9878	0.9915
σ = 0.25	MPSNR(db)	20.1649	32.1479	32.4579	33.8794
	MSSIM	0.5687	0.9104	0.9498	0.9612
	MFSIM	0.8304	0.9735	0.9784	0.9879

Figures-3–4 illustrate the denoising performance in every spectral band of PCA, RAC, and the proposed CS-K-SVD algorithm on Sandi go data, when. Figure-4 shows the comparison of FSIM value among methods in the whole spectrum Sandi go, when. It is found that that the CS-K-SVD method works better than PCA and RAC, no matter what the noise level and testing data are. It demonstrates the rationality of the sparse representation framework and low-rank constraint in our algorithm. Approximation errors may be introduced in the sparse coding and dictionary updating stages in the sparse representation method. These errors could be suppressed by the constraint of low rank. In contrast, the low- rank reconstruction only considers spectral correlation; the performance will be improved when spatial information is considered.

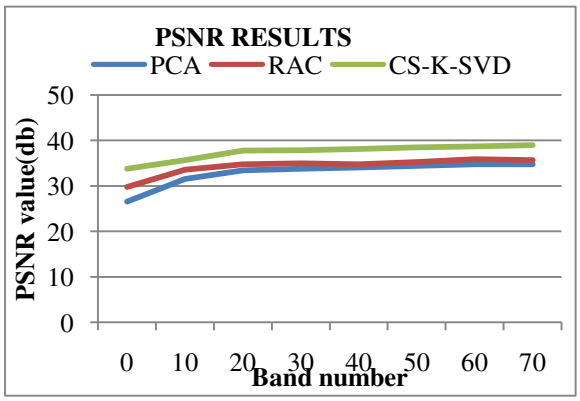

Figure-3. Comparison of PSNR value among methods on spectrum on Sandi go, in the case of σ = 15.

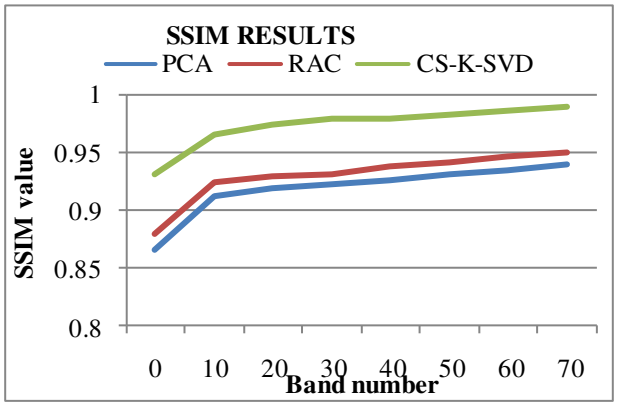

Figure-4. Comparison of SSIM value among methods for whole spectrum on Sandi go, in the case of σ = 15.

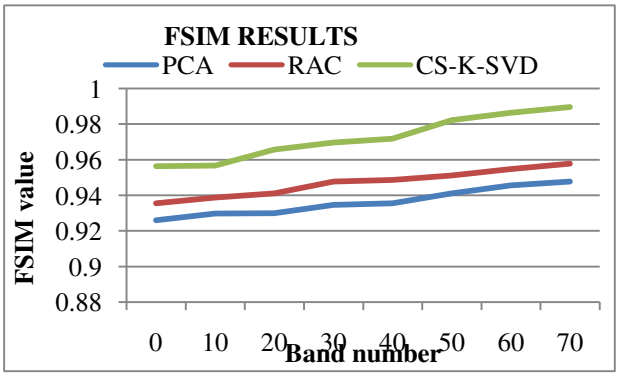

Figure-5. Comparison of FSIM value among methodsin the whole spectrum Sandi go, in the case of σ = 15.

6. CONCLUSIONS AND FUTURE WORK

The hyperspectral image cube can be represented as a three dimensional array. Tensors and the tools of multilinear algebra offer an accepted structure to manage with this kind of mathematical object. Singular value decomposition (SVD) and its variants have been exploited by the HSI community for denoising of hyperspectral imagery. Denoising of HSI with the help of SVD is accomplished by discovering a low rank approximation of a matrix representation of the hyperspectral image cube. This approach of denoising can competently eliminate a variety of mixed or single noise by employing sparse regularization of small image patches. It also preserves the image texture in a comprehensible manner. The learned dictionary exploited clearly assists in eliminating the noise. This paper involved in reducing model to eliminate mixed noise,for instance, Impulse noise, Gaussian-Gaussian mixture and Gaussian-Impulse noise from the HSI data. Excluding theoretical examination, the consistency of combining sparse representation and low rank is also analyzed by means of experimental methods. The experimental results reveal that the denoising method can accomplish competitive performance than other state-of-the-art approaches. The future work will concentrate on considering the gradient in the spectral dimension in the model building process with the intention of developing a real 3-D TV model. Additionally, it might be possible to employ neither the 3-D segmentation nor clustering result to restrict the denoising process from a region perspective, more willingly than the pixel perspective in the present paper.

REFERENCES

[1] Plaza, J. M. Bioucas-Dias, A. Shimic and W. J. Blackwell. 2012. “Foreword to the special issue on hyperspectral image and signal processing,” IEEE J. Sel. Topics Appl. Earth Observ. Remote Sens., Vol. 5, No. 2, pp. 347–353, April.

[2] H. F. Grahn and P. Geladi. 2007. Techniques and Applications of Hyperspectral Image Analysis. Chichester, U.K.: Wiley.

[3] D. G. Goodenough and T. Han. 2009. “Reducing noise in hyperspectral data—A nonlinear data series analysis approach,” in Proc. IEEE WHISPERS’09. 1st Workshop on Hyperspectral Image Signal Process. pp. 1–4.

[4] G. Chen and S. E. Qian. 2011. “Denoising of hyperspectral imagery using principal component analysis and wavelet shrinkage,” IEEE Trans. Geosci. Remote Sens., Vol. 49, No. 3, pp. 973–979, March.

[5] Q. Yuan, L. Zhang and H. Shen. 2012. “Hyperspectral image denoising employinga spectral-spatial adaptive variation model,” IEEE Trans. Geosci.Remote Sens., Vol. 50, No. 10, pp. 3630–3677, October.

[6] H. Othman and S. Qian. 2006. “Noise reduction of hyperspectral imagery using hybrid spatial-spectral derivative-domain wavelet shrinkage,” IEEE Trans. Geosci. Remote Sens., Vol. 44, No. 2, pp. 397–408, February.

[7] G. Chen and S. Qian. 2008. "Simultaneous dimensionality reduction and denoising of hyperspectral imagery using bivariate wavelet shrinking and principal component analysis," Can. J. Remote Sens., Vol. 34, No. 5, pp. 447–454.

[8] B. Goossens, A. Pizurica and W. Philips. 2009. "Image denoising using mixtures of projected Gaussian scale mixtures," IEEE Trans. Image Process., Vol. 18, No. 8, pp. 1689–1702, August.

[9] J. Martín-Herrero. 2007. "Anisotropic diffusion in the hypercube," IEEE Trans. Geosci. Remote Sens., Vol. 45, No. 5, pp. 1386–1398, May.

[10] J. Mairal, M. Elad and G. Sapiro. 2008. "Sparse representation for color image restoration," IEEE Trans. Image Process., Vol. 17, No. 1, pp. 53–69, January.

[11] M. Elad, M. A. T. Figueiredo and Y. Ma. 2010. "On the role of sparse and redundant representations in image processing," Proc. IEEE, Vol. 98, No. 6, pp. 972–982, June.

[12] Kotwal, K. and Chaudhuri S. 2010. Visualization of hyperspectral images using bilateral filtering. Geoscience and Remote Sensing, IEEE Transactions on, Vol. 48, No.5, pp. 2308-2316.

[13] Xu D., Sun L. and Luo J. 2013. Noise estimation of hyperspectral remote sensing image based on multiple linear regression and wavelet transform. Boletim de Ciências Geodésicas. Vol. 19, No. 4, pp. 639-652.

[14] N. Acito, M. Diani and G. Corsini. 2011. Subspace-based striping noise reduction in hyperspectral images. IEEE Trans. Geosci. Remote Sens. Vol. 49, No. 4, pp. 1325–1342.

[15] D. Letexier and S. Bourennane 2008. Noise removal from hyperspectral images by multidimensional filtering. IEEE Trans. Geosci. Remote Sens. Vol. 46, No. 7, pp. 2061–2069.

[16] Karami A., Yazdi M. and Zolghadre Asli A. 2011. Noise reduction of hyperspectral images using kernel non-negative tucker decomposition. Selected Topics in Signal Processing, IEEE Journal of, Vol. 5, No. 3, pp. 487-493.

[17] Zhao, Y-Q. and Jingxiang Yang. 2015. "Hyperspectral Image Denoising via Sparse Representation and Low-Rank Constraint",IEEE transactions on geoscience and remote sensing, Vol. 53, No. 1.

[18] Z. Wang, A. C. Bovik, H. R. Sheikh and E. P. Simoncelli. 2004. "Image quality assessment: From error visibility to structural similarity," IEEE Trans. Image Process., Vol. 13, No. 4, pp. 600–612, April.

[19] L. Zhang, L. Zhang, X. Mou and D. Zhang. 2011. "FSIM: A feature similarity index for image quality assessment," IEEE Trans. Image Process., Vol. 20, No. 8, pp. 2378–2386, August.

[20] M.-D. Iordache, J. M. Bioucas-Dias and A. Plaza. 2012. "Total variation spatial regularization for sparse hyperspectral unmixing," IEEE Trans. Geosci. Remote Sens., Vol. 50, No. 11, pp. 4484–4502, November.